ORIGINAL PAPER

Optical Properties of Cellulose Nanofibre Films at High Temperatures

Ilpo Niskanen[1] · Kaitao Zhang[2] · Mohammad Karzarjeddi[2] · Henrikki Liimatainen[2] · Shuhei Shibata[3] ·
Nathan Hagen[3] · Rauno Heikkilä[1] · Hidehiko Yoda[3] · Yukitoshi Otani[3]

Abstract

Nanocelluloses and their different designs, such as films and nanopapers, have gained considerable interest in many application areas due to their unique properties. For many purposes, such as packaging and electronics, the thermal stability and optical properties of nanocellulose materials are crucial characteristics. In this study, the effects of heat treatment (100 ℃, 150 ℃ and 200 ℃) on the optical and mechanical properties of 2,2,6,6-tetramethylpiperidinyl-1-oxy radical-oxidised cellulose nanofibre (TO-CNF) films were investigated, especially the alteration of the colour, complex refractive index and birefringence. Exposing TO-CNF films to high temperatures (> 150 ℃) induced permanent transformations in the CNF structure, leading to an increase in the refractive index, decreases in the birefringence and crystallinity index, colour darkening and significant deterioration of the mechanical properties.

Introduction

Nanocellulose is a functionalisable renewable biopolymer material that has gained increasing interest in a range of applications relevant to the fields of packaging, technical films and foams, nanocomposites, electronics, photonics, medicines, etc. [1, 2]. In recent years, several new biorefinery concepts have been established to produce cellulose nanomaterials on a larger scale, and the nanocellulose market is expected to grow from US$297 million in 2020 to US$783 million in 2025 [3]. This trend is promoted by the emerging green circular economy, which is based on renewable resources, and by the unique features of nanocellulose, such as its superior mechanical properties, light weight, high surface area, optical transparency, low coefficient of thermal expansion and tailorable chemistry [4, 5].

The thermal stability and alteration of the nanocellulose characteristics under high temperatures are relevant for many applications, such as packaging, composites and electronics [6]. High temperatures (> 100 ℃) can cause changes in the cellulose molecular and crystal structure and can compact the networked structure of cellulose nano-entities. Controlled thermal treatments of solid nanocellulose materials such as films can also be used to improve the mechanical strength (e.g. tensile strength, elongation at break and Young's modulus) [7] and increase the hardness [8] of the films. Typically, the maximum thermal treatment temperature of nanocelluloses is below 200 ℃ because higher temperatures of 200–300 ℃ start to degrade the cellulose polymeric structure [5].

The optical properties of nanocellulose are important parameters for films and nanopapers, and they may also be affected by elevated temperatures (thermal stress) [5]. The optical properties have been commonly investigated by analysing the reflection, absorption, scattering or polarisation of light to obtain different variables, such as transmittance [9], complex refractive index [10], optical activity [11], colour [12], birefringence [13], opacity [14] and gloss [15].

Birefringence arises from the asymmetric nature of structures within many transparent optical materials, such as nanocelluloses. The birefringence of a material is defined as the difference between extraordinary and ordinary refractive

✉ Ilpo Niskanen
Ilpo.Niskanen@oulu.fi

1 Faculty of Technology, Structures and Construction Technology, University of Oulu, P.O. Box 7300, 90014 Oulu, Finland

2 Faculty of Technology, Fibre and Particle Engineering, University of Oulu, P.O. Box 4300, 90014 Oulu, Finland

3 Graduate School of Engineering, Utsunomiya University, 7-1-2 Yoto, Utsunomiya, Tochigi 321-8585, Japan

indices. This depends on the wavelength, as different wavelengths interfere to different extents with the atoms of the material. Changes in the birefringence of material mean that significant changes have occurred within the structure of the material [16].

The refractive index is a fundamental property of a material and is useful in many areas of science and engineering. The value of the refractive index is affected by magnetic permeability, dielectric permittivity and conductivity of the material [17]. Thus, it has been widely used in the quality inspection of liquids and solids and in material science to characterise minerals, such as the detection of material concentration, purity, chemical identification of species, density and even temperature [18]. Information on the refractive index is often associated with the material's visual appearance through scattering and reflection properties; it is a key parameter in the design of optical systems. In addition, refractive index values are required when calculating the dimensions of nanocrystals, for example, by the Mie theory or Rayleigh approximation equations [10]. Therefore, refractive index data for various (pure) materials have been determined and exist in common physics and chemistry handbooks.

The refractive indices of nanocelluloses are typically affected by differences in the birefringence, degree of crystallinity, state of purity and source. Therefore, the refractive index can also be used as a quality parameter. The knowledge of the transformation of the optical characteristics of nanocellulose materials as a function of temperature is still incomplete, and previous studies have mainly addressed the colour of cellulose nanomaterials [4]. The existing literature does not report the refractive index of cellulose nanofibres (CNFs) as a function of wavelength; instead, it only determines the index at a single wavelength. In addition, the alteration of the refractive index during the heat treatment of nanocellulose materials has not been reported. We hypothesise that optical properties, such as birefringence and refractive index, are affected by thermal stress and can be controlled by conditions of heat treatments. The optical parameters may also be used to estimate the deterioration (changes) of mechanical properties.

In our previous work, we developed a method for determining the complex refractive index of cellulose nanocrystals (CNCs) as a function of wavelength by combining the Beer–Lambert and immersion-matching methods [10]. The sizes of the nanocelluloses (CNCs and CNFs) were, in turn, analysed using Rayleigh approximation and the Mie theory [19]. The change in the birefringence properties of the thermally modified wood was obtained by measuring light reflection with a Stokes imaging polarimeter based on the Mueller matrix method [20]. The present study aims to investigate the optical (colour, complex refractive index and birefringence), structure (degree of crystallinity, thermal stability and chemical bonds) and mechanical (tensile strength, strain and Young's modulus) properties of heat-treated films of 2,2,6,6-tetramethylpiperidinyl-1-oxy radical-oxidised cellulose nanofibres (TO-CNFs) and to provide a further understanding of the behaviour of nanocellulose films at elevated temperatures (100–200 ºC).

Materials and methods

Materials

Bleached birch (Betula pendula) chemical wood pulp obtained in dry sheets was used as a cellulose raw material after being disintegrated in deionised water. The properties of birch pulp were determined in a previous study [21]. The cellulose, xylan and glukomannan contents of the pulp were 74.8%, 23.6% and 1.1%, respectively. The 2,2,6,6-tetramethylpiperidinyl-1-oxy radical (TEMPO), sodium bromide and sodium hypochlorite solution (NaClO, 15 wt%) were obtained from Sigma–Aldrich (Finland).

Preparation of TEMPO-oxidised CNFs (TO-CNFs)

The cellulose pulp was subjected to TEMPO-mediated oxidation, mechanical delamination treatment and purification. TEMPO-mediated oxidation was performed as previously described [21]. In the present study, 10 mmol NaClO per gram of pulp fibre was used to achieve a charge density of 1.0 mmol/g. After oxidation and washing with water (until the conductivity of the filtrate was already below 20 µS/cm), a suspension with a 0.6% dry-matter content was prepared and was delaminated via probe sonication for 1 h (Heilscher UP 400S, 0.5 s power discharge and 0.5 s pause, 60% amplitude and 22 mm probe tip diameter) to obtain TO-CNFs. To remove the larger fibres and metal dust generated from the sonication probe and to obtain an aqueous TO-CNF suspension, the sample was centrifuged at 8,000 rpm for 10 min.

Preparation of TO-CNF films

TO-CNF films were prepared via casting. The TO-CNF suspension was degassed overnight using a vacuum, poured into a polystyrene Petri dish and dried with 50% humidity at room temperature for more than one week. The obtained self-standing TO-CNF films were heat-treated in an oven for 3 h at 100 ºC, 150 ºC and 200 ºC, respectively. The thicknesses of the TO-CNF films (reference non-treated TO-CNF film and TO-CNF films heat-treated at 100 ºC, 150 ºC and 200 ºC, respectively) measured via scanning electron microscopy were 27.7, 28.2, 27.6 and 28.1 µm, respectively.

Characterisation of the TO-CNF films

Colorimeter

The colour of the TO-CNF films was measured with a spectrophotometer (Lorentzen & Wettre Elrepho 070) under a D65 light source. The colour analysis was based on the CIE 1976 L*a*b* (CIELAB) colour space. The colour was defined by the parameters L* = lightness (or clarity) of the colour (L* = 0 yields black and L* = 100 yields white), a* = position between magenta and green (green indicates negative values and magenta, positive) and b* = position between yellow and blue (blue indicates negative values and yellow, positive). The colour difference ΔE between two colour stimuli was calculated as the Euclidean distance between the points representing them in the L*a*b* colour space [4, 22]. The values of ΔE between 0.5 and 1 in colour difference can already be perceived by the human eye. The total colour differences ΔE_ab^* were calculated using the following formula:

$$\Delta E_{ab}^* = \sqrt{\Delta L^{*2} + \Delta a^{*2} + \Delta b^{*2}}, \tag{1}$$

where $\Delta L^* = L^* - L_0^*$, $\Delta a^* = a^* - a_0^*$ and $\Delta b^* = b^* - b_0^*$. L^* is the lightness, and a^* and b^* are the colour coordinates under the testing conditions. L_0 is the reference value of lightness, and a_0 and b_0 are the reference values of the colour coordinates, respectively.

Spectroscopic photometry

The optical properties of any material can be described by the complex refractive index:

$$N(\lambda) = n(\lambda) - ik(\lambda), \tag{2}$$

where λ is the wavelength, k is the extinction coefficient and n is the real refractive index. The refractive index is defined as the speed of light in a vacuum divided by the speed in the medium. The extinction coefficient (imaginary part) is therefore described as the reciprocal damping of the oscillation amplitude of the incident electric field in the medium [17]. The complex refractive index was determined as the absolute (500–1000 nm) unpolarised reflectance $R_0(\lambda)$ and transmission $T_0(\lambda)$ that is spectrally resolved from the TO-CNF films using a Jasco V-670 with an ARMN-735 absolute-reflectance measurement accessory at a 5° angle of incidence. In mathematical form, this is expressed as follows:

$$R_0 = \frac{(n_0 - n_s)^2 + k^2}{(n_0 + n_s)^2 + k^2}. \tag{3}$$

and

$$T_0 = \frac{4\sqrt{n_s^2 + k^2}}{(1 + n_s)^2 + k^2}, \tag{4}$$

where n_0 is the refractive index of the medium, n_s is the refractive index of the film and κ is the extinction coefficient of the film. Generalising this result to the bulk sample's polarised reflectance and transmittance, Rs and Ts can be defined as follows:

$$= R_0 + \frac{T_0^2 R_0 T_v^2}{1 - R_0^2 T_v^2}. \tag{5}$$

and

$$T_s = \frac{T_0^2 T_v}{1 - R_o^2 T_v^2}, \tag{6}$$

where T_v is the transmittance through the volume. T_v can be expressed as follows:

$$T_v = \exp(-4kd/\lambda), \tag{7}$$

where d is the thickness of the film. Using spectrally resolved bulk sample reflectance and transmission, we estimated the (n, k) model parameters as a function of the wavelength using least-squares fitting to solve the complex refractive index of the film [23, 24].

Polarimeter

The retardance (δ) is a measure of the phase shifts when linearly polarised components of light pass through a material. The linear retardance of the TO-CNF films in this study was determined using an Axoscan Mueller matrix polarimeter (Axometrics, USA). The spectra (550–800 nm) were measured at intervals of 1.0 nm. The polarisation properties of the TO-CNF films were obtained from the decomposition analysis of the Mueller matrix with a dual-rotating retarder system, and the polarisation property images were obtained by moving the sample through an XY motor stage (range: 200×200 mm; resolution: 1 mm). The birefringence (Δn) optically anisotropic film is obtained from the following expression

$$\Delta n(n_o - n_e) = (\delta \bullet \lambda)/(2\pi \bullet d), \tag{8}$$

where δ is the retardance, λ is the wavelength, n_o is the ordinary refractive index, n_e is the extraordinary refractive index and d is the film thickness [25].

Transmission Electron Microscopy (TEM)

The morphological features of the TO-CNFs were observed using a transmission electron microscope (TEM, JEOL

JEM-2200FS, Japan). Preparation of the samples was performed by first adding a small droplet of 0.003 to 0.005 wt% nanocellulose suspension on top of the carbon-coated copper grid. After setting for one minute, the sample was absorbed by a small piece of filter paper, and the sample left on the grid was negatively stained with uranyl acetate (2% w/v) for 1 min. The staining agent was then removed again with filter paper. Standard conditions of 200 kV were used during the TEM analysis.

Field Emission Scanning Electron Microscopy (FESEM)

FESEM images of the films were obtained using a field emission scanning electron microscope (Zeiss Sigma HD VP, Oberkochen, Germany) at a 0.5 kV acceleration voltage. All samples were sputtered with platinum before observation.

Contact Angle (CA) Measurement

CA measurements were conducted using Krüss-DSA25 (Germany). A small drop of deionised water was dosed automatically using the glass syringe on a fixed and dried film; measurements were recorded for 30 s. The results were presented as an average of at least five measurements.

X-ray Diffraction (XRD)

The XRD patterns of the samples were recorded using a Rigaku SmartLab 9 kW XRD machine. The analysis involved the following parameters: $K\alpha$ radiation ($K_{\alpha1} = 1.78892$ Å; $K_{\alpha2} = 1.79278$ Å; $K_{\alpha1}/K_{\alpha2} = 0.5$) and a scan rate of 3°/min between 10° and 50° 2θ and 0.02°/step size. The crystallinity index (C_{rI}, %) was calculated as follows:

$$C_{rI}(\%) = \frac{I_{200} - I_{am}}{I_{200}} 100, (9).$$

where I_{200} is the maximum intensity of the principal peak and I_{am} is the intensity of the diffraction attributed to non-crystalline cellulose.

Diffuse Reflectance Infrared Fourier Transform (DRIFT) Spectroscopy

Chemical characterisation of the films was carried out using DRIFT spectroscopy. The spectra were recorded on a Bruker Vertex 80v spectrometer (USA) in the 800–4,000 cm^{-1} range with a 2 cm^{-1} resolution.

Thermogravimetric Analysis (TGA)

TGA was performed using a thermal analyser (TA Instruments SDT 2960) under nitrogen flow with a constant rate of 60 mL min^{-1}. Each measurement was conducted from 30 to 1,000 °C at a scanning rate of 10 K/min.

Degree of Polymerisation (DP)

The ISO5351 standard method was applied to measure the DP of the film samples. The limiting viscosity number ([μ]) of the dried samples (0.15–0.2 g) was determined using a capillary viscometer by dissolving the samples in 50 mL of 0.5 M cupriethylene diamine and then measuring the viscosity using the standard testing procedure. The viscosity average DPv value was calculated according to a previously reported equation [26]:

$$(DPv^{0.905} = 0.75[\mu]) \tag{10}$$

Mechanical properties

The mechanical properties (tensile strength, elongation at break and Young's modulus) of the TO-CNF films were determined using a universal testing machine (Zwick D0724587, Switzerland) equipped with a 1 kN load cell. The Young's modulus was obtained by determining the slope of the tensile strength–strain curves. All samples were cut into 5-mm-wide strips and placed at 23 ± 1 °C with a relative humidity of $50 \pm 2\%$ for at least 24 h. The thickness of each specimen was determined using a precision thickness gauge (Hanatek, FT3, St. Leonards-on-Sea, UK), with the average value obtained from three random locations on the sample strip. For the TO-CNF film heat-treated at 200 °C, the average thickness of the film before heat treatment was chosen because of the small bubbles that were found on the film surface after heating. The initial grip separation of the machine was set at 20 mm, and the specimens were tested at a constant crosshead speed of 5 mm/min. At least five specimens were tested, and the average value obtained was reported.

Results

Colour changes in the thermally modified TO-CNF films

Figure 1 presents the original, untreated TO-CNF film (reference) and the films heat-treated at 100 ℃, 150 ℃ and 200 ℃, respectively, in an oven. The alteration of the visual appearance of the films heat-treated at 150 ℃ and 200 ℃ is clearly perceived with the naked eye: the colour of the films changes from transparent to light brown as the temperature increases. The yellow or brown film discolouration provides a near-complete UV-blocking ability
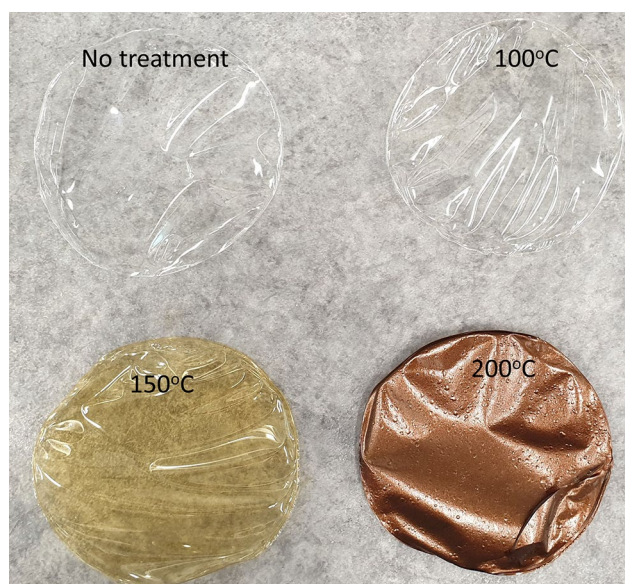
Fig. 1 Reference and heat-treated TO-CNF films (100, 150, 200 °C) with 3 h treatment time

Fig. 2 Changes in total colour difference (ΔE*) of the reference and heat-treated TO-CNF films as a function of treatment temperature

[2]. Thermal discolouration has been attributed to the carbonyl and carboxyl functional groups of pure (lignin- and hemicellulose-free) cellulose, which can initiate the formation of chromophores, especially in oxidised cellulose nanomaterials such as mediated TEMPO [26].

Figure 2 shows the changes in the total colour difference (ΔE*) of the films. The ΔE* values of the samples heat-treated for 3 h at 100 °C, 150 °C and 200 °C are 1.6, 37.8 and 69.4, respectively; that is, the ΔE* values show a nonlinear dependence on the heat treatment temperature and indicate only minor changes below 100 °C, but notable discolouration is observed above 150 °C. Previously, thin CNF films produced using only mechanical treatment had ΔE* values of 6.1, 6.6, 7.3 and 10.5 at 80 °C, 120 °C, 160 °C and 190 °C (calculated from the figure), respectively [4]. Therefore, the TO-CNFs in the current work (charge density: 1.0 mmol/g) are significantly more prone to thermal discolouration. The oxidised groups in cellulose (i.e. CO and COOH) have been generally noted to promote yellowing. In particular, carbonyl groups initiate the formation of chromophores, which are formed later, upon yellowing. Carboxyl groups, in turn, have a strong synergetic role when carbonyl groups are present, and they promote acidic catalysis and additional activation by electronic effects [27]. In particular, the C2 and C3 ketones and aldehyde groups that can be formed due to side reactions have been previously reported to cause brown discolouration for the TEMPO-oxidised nanocellulose [28].
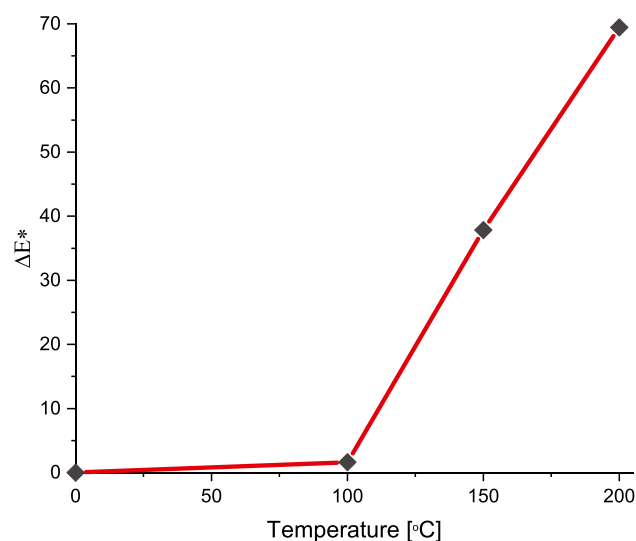
Complex refractive index of the thermally modified TO-CNF films

The influence of heat treatment on the complex refractive index of the TO-CNF films as a function of wavelength is shown in Fig. 3. Figure 3a presents the real effective refractive index spectra of the film samples. The refractive index of an untreated CNF has not been previously reported as a function of wavelength; only the value of a single 785 nm wavelength was available, with a refractive index of 1.458 [29]. The refractive index estimate obtained by our method is $n_{785} = 1.454$; it matches the literature value very well. The magnitude of the real refractive indices of all the TO-CNF films slightly decreased or stayed at a constant level as a function of the wavelength of light, except that of the film heat-treated at 200 °C (Fig. 3a). This behaviour is attributed to the absorption of the visible part of the incident light for the dark film interface. Hence, in such cases, light reflection usually becomes weak. The effective refractive indices of the thermally modified TO-CNF films increased as a function of treatment temperature (Fig. 3a). According to these results, the values of the ordinary refractive indices increased with a decrease in the extraordinary refractive index values as the temperature increased. The same phenomenon was observed earlier for heat-treated pinewood [30]. The refractive indices of the original Scots pine (no treatment) and thermally modified wood treated at 180 °C, 200 °C and 230 °C were 1.553, 1.557, 1.587 and 1.596 at 589 nm, respectively, obtained using the liquid immersion technique. As indicated, the refractive index of the Scots pine treated at 230 °C approached the maximum ordinary refractive index of cellulose (i.e. 1.596 at 589 nm).
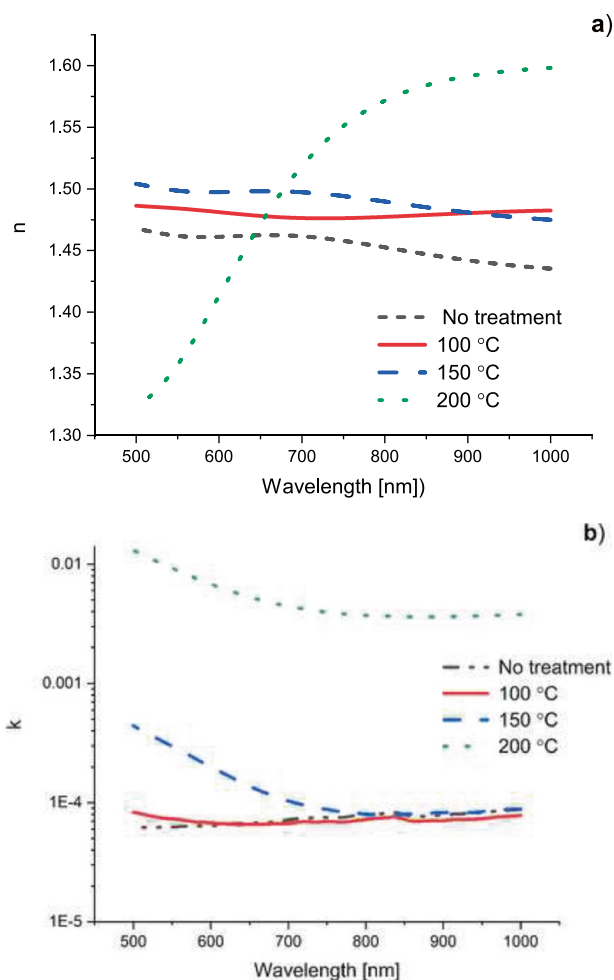
Fig. 3 Real (**a**) and imaginary (**b**) parts of the complex refractive indices of the reference and heat-treated TO-CNF films

Fig. 4 (**a**) Linear retardance and (**b**) birefringence of the reference and heat-treated TO-CNF films as a function of the wavelength

Similarly, the highest heat treatment (200 ℃) of the TO-CNF film resulted in a refractive index of 1.598 at 1,000 nm.

The behaviour of the imaginary part of the complex refractive index curves is shown in Fig. 3b) as a function of the wavelength. Significant values of the imaginary part of the complex refractive index are observed only at the higher heat treatment temperatures (150 ℃ and 200 ℃). The imaginary part of the refractive index for the reference (untreated) film and the film heat-treated at 100 ℃ is about 0.0001, without large wavelength dependence. For films, extinction coefficients below 0.0001 are generally considered negligible, and low values of the imaginary component of the complex refractive index correspond to high optical transparency.

Birefringence of the thermally modified TO-CNF films

Figure 4 shows the spectral dispersion curves of linear retardance and the birefringence (Δn) obtained using optical
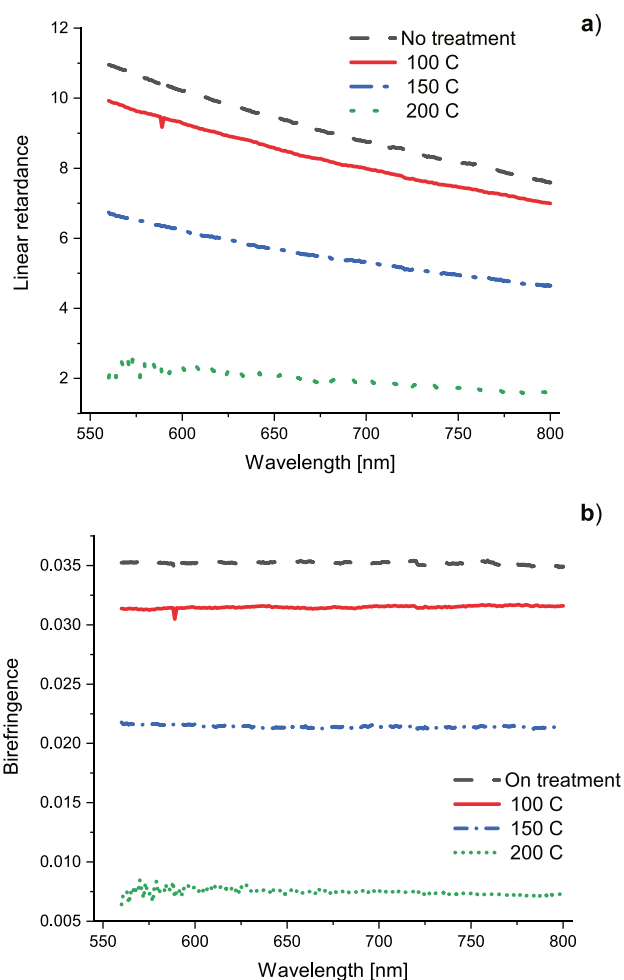
anisotropy. The birefringence decreased with increasing heat treatment temperatures. The birefringence of optically anisotropic materials, such as cellulose, is considered a measure of the relative area occupied by non-crystalline and crystalline regions [31]. The decreasing birefringence with the increase in heat treatment temperature indicates that the birefringence has disappeared; as a result, the structure of the CNF starts to degrade. This influences the mechanical properties of the CNF [32]. Birefringence provides information about the whole molecular structure of cellulose, whereas XRD mainly provides orientation information about the crystals [31]. The birefringence of cellulose measured from bacterial CNF films was previously reported to range from 0.047 to 0.090 [30], depending on the differences in the treatment, state of purity, source, wavelength, measurement temperature and measurement method used. In our samples, birefringence was measured at 0.035, which is slightly lower than the values in the literature. At the highest heat treatment temperature (200 ℃), the birefringence value decreased to

0.0075. Degushi, Tsujii and Horikoshi investigated the birefringence of the water suspension of cellulose fibres using an ellipsometer [33]. They observed that the birefringence of cellulose was completely lost at 330 °C and at a constant pressure of 25 MPa.

Microstructure and contact angle of the TO-CNF films

Figure 5 shows the TEM image and width distribution graph of TO-CNF, FESEM images of original TO-CNF and thermal-treated TO-CNF films. TO-CNFs are flexible and elongated nanofibrils with an average length ranging from 172 to 958 nm and a width of 5 ± 2 nm. Both the reference (untreated) film and the films heat-treated at 100 °C and 150 °C have a smooth and non-porous surface, while small particles and holes are observed on the surface of the film heat-treated at 200 °C. These micro- and nano-sized holes probably appear as a result of the agglomeration of nano-sized cavities between the cellulose molecular chains [34]. Moreover, crevices appear in the cross-section areas and become larger with higher temperatures, indicating notable changes in the microstructure of the nanofibre network.

The possible changes in the film surface characteristics induced by heat treatment were revealed in terms of surface CA (Table 1). The reference film and the films treated at 100 °C and 150 °C possessed a typical CA of CNF films, ranging

Table 1 Contact angle (CA) and DPv values for the reference and heat-treated TO-CNF films

Sample	Mean CA(m) [°]	DPv
No treatment	59.1	142.1
100 °C	66.9	169.6
150 °C	67.3	108.0
200 °C	35.3	65.2

from ~ 59° to 67°. A significant decrease in CA was observed at 200 °C (CA of 35°), indicating that the hydrophilicity of the film surface increased notably. This decrease in CA was presumably associated with the formation of hydrophilic groups (e.g. C2 and C3 ketones and aldehyde groups) caused by thermal degradation. Moreover, the alteration of the surface structure by the creation of small particulates and micro- and nano-sized holes, as observed in the FESEM analysis, may have contributed to the CA.

Crystalline structure of the thermally modified TO-CNF films

Crystallinity has a significant effect on the physical, optical and mechanical properties of cellulose materials. Figure 6 depicts the XRD patterns of the films treated at different temperatures in this study. The crystallinity of CNF films was 58.4%, 56.4%, 57.3%, and 45.6% for the reference film
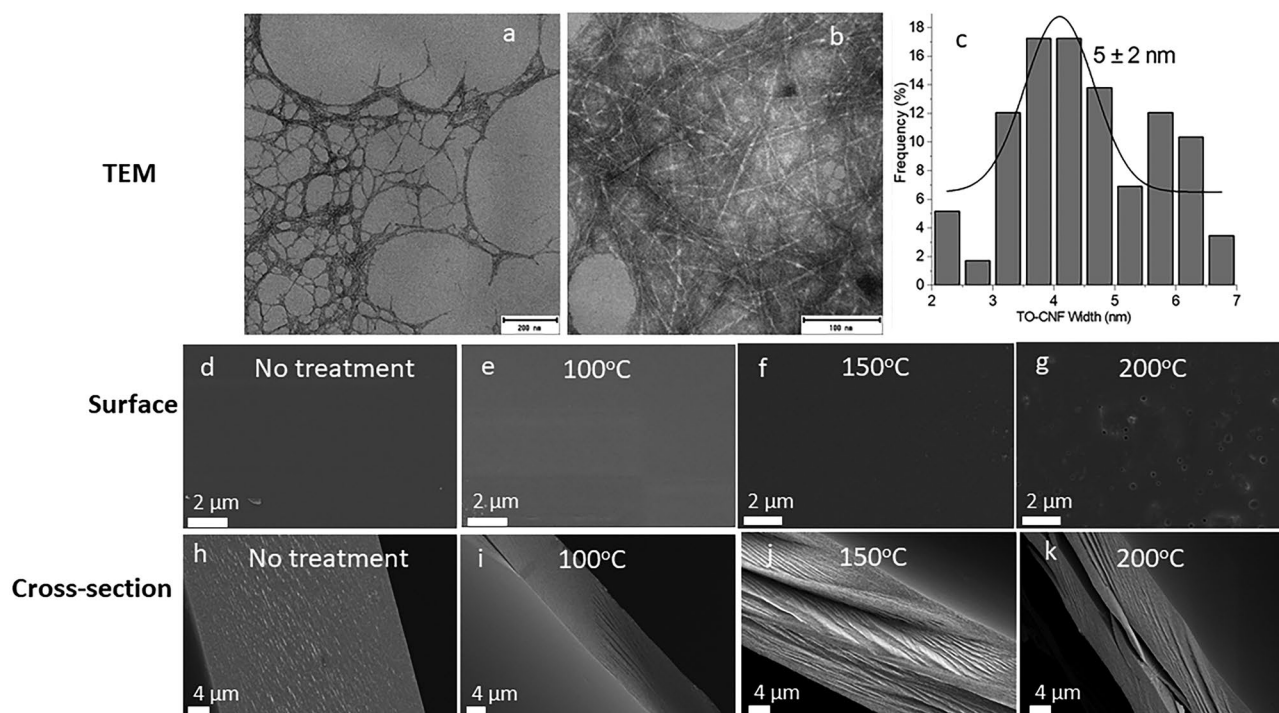

Fig. 5 TEM image and width distribution graph of TO-CNFs and FESEM images of the surfaces (**d–g**) and cross-sectional areas (**h–k**) of the reference and heat-treated TO-CNF films
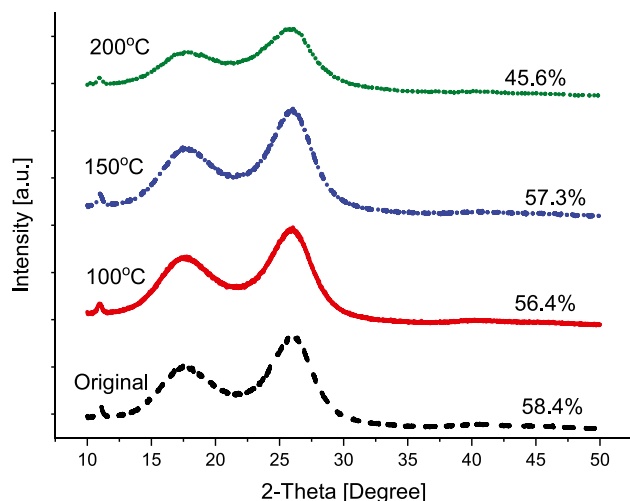
Fig. 6 X-ray diffractograms and crystallinity indices of the reference and heat-treated TO-CNF films

Fig. 7 DRIFT spectra of the reference and heat-treated TO-CNF films

and for the films heat-treated at 100 ℃, 150 ℃ and 200 ℃, respectively. All of the films displayed typical cellulose I peaks, with the main 2θ diffraction angles at approximately 18.5 and 26° (Co Kα radiation source) [35]. The results indicated that the crystalline form (allomorph) of the cellulose remained unchanged during the heat treatment. For the films heat-treated at 100 °C and 150 °C, their crystallinity indices (C_{rI}) decrease only slightly, indicating high crystalline ordering and good stability. However, for the film heat-treated at 200 °C, the C_rI decreases dramatically (from 58.4% to 45.6%); this is an effect associated with the degradation of the molecular ordering and polymeric structure of cellulose.

Chemical analysis of the thermally modified TO-CNF films

Figure 7 shows the DRIFT spectra of the TO-CNF films in this study. All the DRIFT spectra of the TO-CNF films show typical characteristics of cellulose and similar chemical structures. The absorption peaks in the region between 3,350 and 3,740 cm^{-1} are due to O–H stretching vibrations. The peaks at around 2,903 cm^{-1} are associated with C–H stretching vibrations. Overall, the heat treatment appears to have limited influence on the chemical structure of TO-CNF films except for the peak at 1640 cm^{-1} and a newly appearing band at 1740 cm^{-1}. Notably, the peak at around 1,640 cm^{-1} is characteristic of the sodium carboxylate group originating from TEMPO-mediated oxidation. This peak shifts to a lower wavenumber value with a higher heat treatment temperature, which is probably related to the formation of intra- and interfibrillar hydrogen bonds promoted by heat treatment [36]. Additionally, a new band at around 1,740 cm^{-1} appears as the treatment temperature increases,
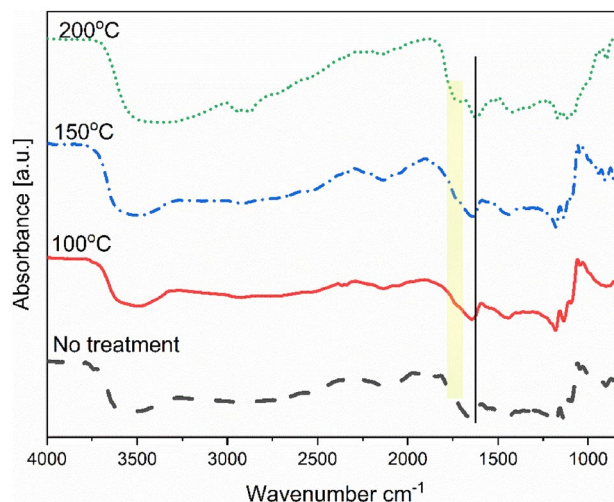
which can probably be ascribed to the carbonyl bonds in chromophore groups formed during the heat treatment [34].

Thermogravimetric analysis and degree of polymerisation of the thermally modified TO-CNF films

The results of the thermogravimetric analysis (TGA) of the heat-treated films are shown in Fig. 8. All films exhibited the typical three weight-loss stages of nanocellulosic materials. The weights of all the samples that were heat-treated at temperatures under 200 °C decreased slightly due to the evaporation of the absorbed water. As expected, this water loss decreased as a function of the heat treatment temperature because of the reduction in the residual water in the films. The second weight corresponding to the thermal degradation of the sodium carboxylates starts at approximately 200 °C. Moreover, it can be noted that the film heat-treated at 200 °C shows a higher thermal degradation point compared to the untreated film. Due to the thermal-oxidative decomposition of the char, a third weight loss is observed when the temperature is higher than 300 °C [37]. Additionally, the amount of char at 1,000 °C is 23.3% for the untreated film, 23% for the film heat-treated at 100 °C, 25.6% for the film heat-treated at 150 °C and 30.2% for the film heat-treated at 200 °C. The higher amounts of char in the heat-treated films are reasonable because the weight loss or decomposition of the films already occurred during the heat treatment, before the TGA measurement. The temperatures at the maximum weight losses of the reference film and the films heat-treated at 100 ℃, 150 ℃ and 200 ℃ are determined to be 241.2 ℃, 241.6 ℃, 241.9 ℃ and 294.1 ℃, respectively.
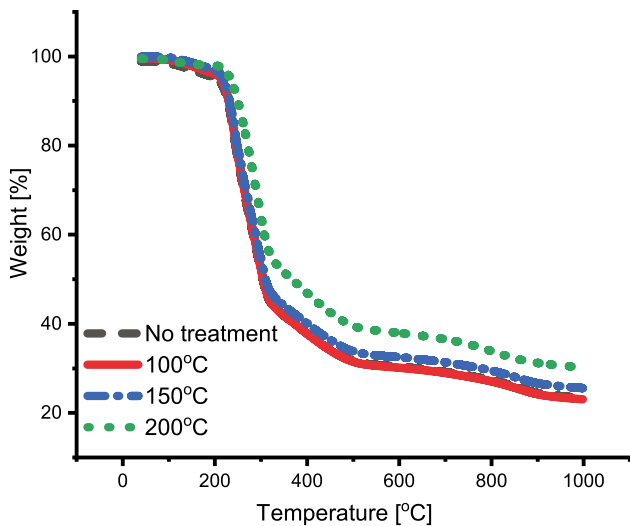
Fig. 8 Weight losses of the reference and heat-treated TO-CNF films

The influence of heat treatment on the degree of polymerisation of the TO-CNF was revealed using a method based on limiting the viscosity number. A slight increase in DP was observed when the film was treated at 100 °C, likely due to evaporation of moisture and possible chemical residues, while a notable decrease in DP was noted at higher temperatures (Table 1). In particular, the high temperature of 200 °C resulted in significant degradation of the TO-CNF structure, which was also indicated by the crystallinity values.

Mechanical properties of the thermally modified TO-CNF films

The mechanical properties of the TO-CNF films in this study, as measured with a universal testing machine, are presented in Fig. 9. All the TO-CNF films except the film heat-treated at 200 ℃ were easy to handle and flexible when
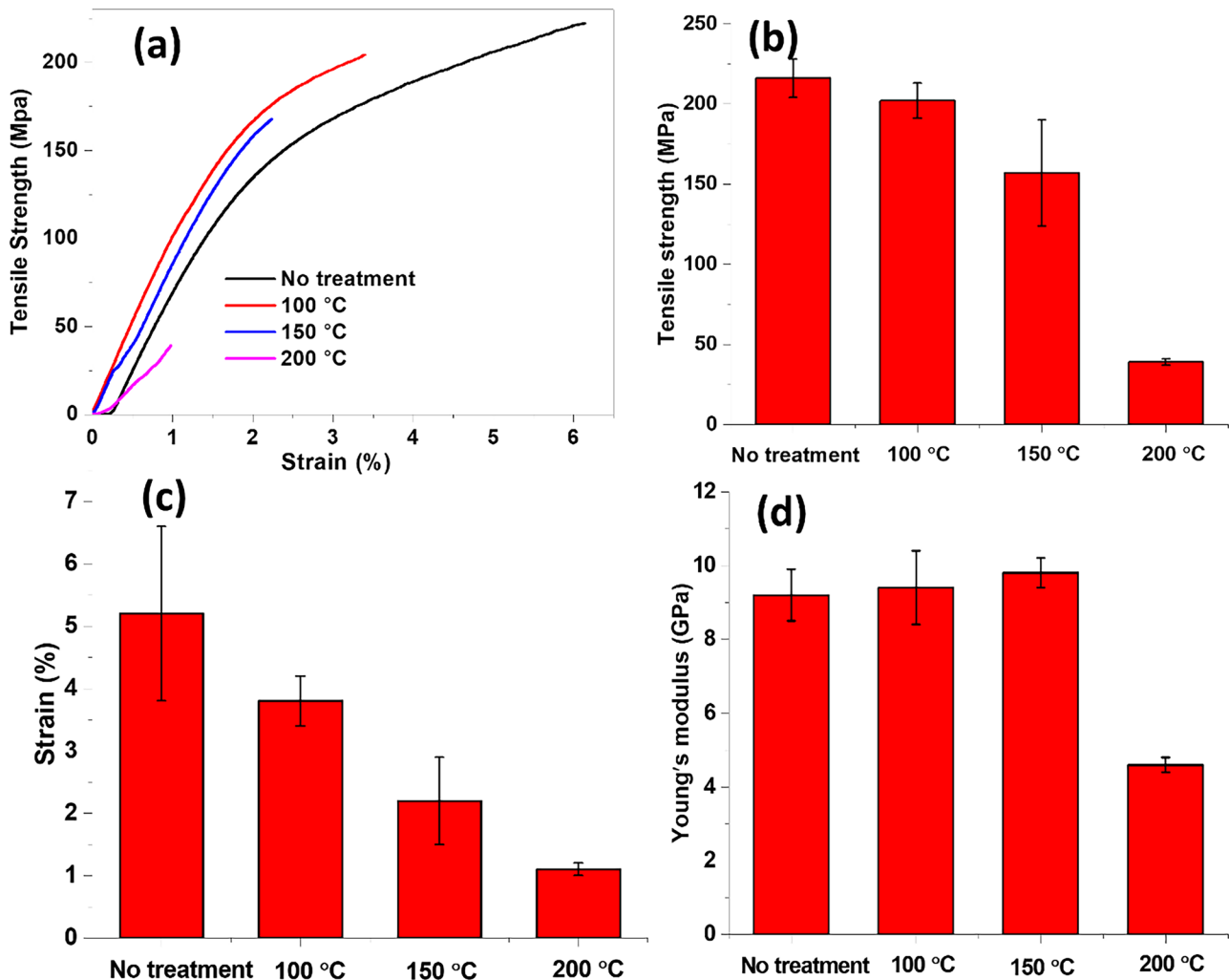

Fig. 9 (**a**) Typical tensile strength–strain curves and tensile strength (**b**), strain (**c**) and (**d**) Young's modulus of the TO-CNF films heat-treated at different temperatures

bent. Both the tensile strength and the strain display a gradual decrease as a function of the heat treatment temperature, already starting at 100 ℃. However, the decrease in strength and elongation is small at 100 ℃, when the tensile strength is still > 200 MPa and the strain is > 3.5%. At higher temperatures, the decrease in strength and strain was notable.

The Young's modulus, in turn, showed a slight increase as a function of the treatment temperature (from 9.2 to 9.8 GPa) until 200 ℃. This increase in stiffness can be attributed to the formation of intra- and interfibrillar hydrogen and carbonyl bonds due to heat treatment (Fig. 7). The TO-CNF film heat-treated at 200 ℃ had some small bubbles on its surface, and the film became more brittle and easier to break. Thus, the mechanical properties of the film heat-treated at 200 ℃ drop dramatically: the tensile strength is only 39 ± 2 MPa (82% decrease compared to the reference film), the strain is 1.1 ± 0.1% (79% decrease) and the Young's modulus is 4.6 ± 0.2 GPa (50% decrease). The reduction of the mechanical properties at higher temperatures is mainly attributable to the decrease in the degree of polymerisation of TO-CNF and to the destruction of the crystalline structure of TO-CNF's crystalline structure [2]; both decreased the mechanical strength of the individual nanofibres.

Conclusion

The role of thermal stress in the molecular structure of cellulose and nanocellulose is well known and reported in the literature. However, a basic understanding of the optical characteristics of nanocellulose films at elevated temperatures is lacking despite the fact that these are crucial properties in numerous applications. In the present study, our results provide a deeper understanding of the mechanisms of CNF restructuring after the heat treatment process and their impact on the optical and mechanical properties of TO-CNF films.

Some important findings are summarised as follows: The films were colourless at the low heat treatment temperatures (< 100 ℃), but significant discolouration was noted at the higher temperatures (> 100 ℃). The refractive indices of the thermally modified TO-CNF films increased significantly as a function of the treatment temperature. The highest heat treatment (200 ℃) of the TO-CNF film resulted in a refractive index of 1.598; in this case, the film approached the maximum ordinary refractive index of cellulose (1.596). A higher refractive index improves the appearance of the film. The polarimeter test showed that the birefringence decreased with increasing heat treatment temperatures and that the birefringence of nanocellulose was nearly completely lost at 200 ℃. Small particles and holes were observed on the surface of the film heat-treated at 200 ℃. In addition, crevices appeared in the cross-section areas, indicating notable changes in the microstructure of the nanofibre network. The crystallinity indices decreased only slightly at 100 ℃ and 150 ℃, indicating high crystalline ordering and good stability, but at 200 ℃, the crystallinity indices decreased dramatically, which was associated with the degradation of the molecular ordering and polymeric structure of cellulose. The higher thermal stability of the sample heat-treated at 200 ℃ can be related to its lower crystallinity, which produces slow heat transferability. The films heat-treated at high temperatures presented lower weight loss in the TGA, especially the films heat-treated at 200 ℃, but they also exhibited a significant decrease in crystallinity. The tensile strength and strain displayed a gradual decrease as a function of the heat treatment temperature and made the films brittle. Young's modulus, in turn, showed a slight increase as a function of the treatment temperature until 200 ℃. At higher temperatures, the decrease in strength, strain and Young's modulus was notable. These factors may limit the suitability of the TO-CNF films for applications and are presumably affected by the oxidised groups in cellulose (i.e. CO and COOH) formed during the TEMPO treatment.

To conclude, the birefringence and refractive index information can potentially be harnessed to predict the mechanical properties of nanocellulose and to evaluate the change in the nanofibre structure as a function of temperature.

Declarations

Conflict of interest The authors declare that they have no conflict of interest.

References

1. Abitbol T, Rivkin A, Cao Y, Nevo Y, Abraham E, Ben-Shalom T, Lapidot S, Shoseyov O (2016) Nanocellulose, a tiny fiber with

huge applications. Curr Opin Biotechnol. https://doi.org/10.1016/j.copbio.2016.01.002

2. Yang W, Gao Y, Zuo C, Deng Y, Dai H (2019) Thermally-induced cellulose nanofibril films with near-complete ultraviolet-blocking and improved water resistance. Carbohydr polym. https://doi.org/10.1016/j.carbpol.2019.115050

3. Nanocellulose market, Report code CH3320. Published, https://www.marketsandmarkets.com/Market-Reports/nano-cellulose-market-56392090.html.Mar 2020 Accessed 20 Aug 2021

4. Pakharenko V, Sameni J, Konar S, Pervaiz M, Yang W, Tjong J, Oksman K, Sain M (2021) Cellulose nanofiber thin-films as transparent and durable flexible substrates for electronic devices. Mater & Design. https://doi.org/10.1016/j.matdes.2020.109274

5. Gan PG, Sam ST, Abdullah M, Omar MF (2020) Thermal properties of nanocellulose-reinforced composites: A review. J Appl Polym Sci

6. Agustin MB, Nakatsubo F, Yano H (2016) The thermal stability of nanocellulose and its acetates with different degree of polymerization. Cellulose. https://doi.org/10.1007/s10570-015-0813-x

7. Rubentheren V, Ward TA, Chee CY, Nair P, Salami E (2016) Effects of heat treatment on chitosan nanocomposite film reinforced with nanocrystalline cellulose and tannic acid. Carbohydr Polym. https://doi.org/10.1016/j.carbpol.2015.12.068

8. Wu Q, Meng Y, Concha K, Wang S, Li Y, Ma L, Fu S (2013) Influence of temperature and humidity on nano-mechanical properties of cellulose nanocrystal films made from switchgrass and cotton. Ind Crops Prod. https://doi.org/10.1016/j.indcrop.2013.03.032

9. Sun X, Wu Q, Zhang X, Ren S, Lei T, Li W, Xu G, Zhang Q (2018) Nanocellulose films with combined cellulose nanofibers and nanocrystals: tailored thermal, optical and mechanical properties. Cellulose. https://doi.org/10.1007/s10570-017-1627-9

10. Niskanen I, Suopajärvi T, Liimatainen H, Fabritius T, Thungström G (2019) Determining complex refractive index of cellulose nanocrystals by combination of Beer-Lambert and immersion matching methods. J Quant Spectrosc Radiat Transf. https://doi.org/10.1016/j.jqsrt.2019.06.023

11. Zlenko DV, Nikolsky SN, Vedenkin AS, Politenkova GG, Skoblin AA, Melnikov VP, Michaleva MM, Stovbun SV (2019) Twisting of fibers balancing the gel-sol transition in cellulose aqueous suspensions. Polym. https://doi.org/10.3390/polym11050873

12. Vardanyan V, Galstian T, Riedl B (2015) Effect of addition of cellulose nanocrystals to wood coatings on color changes and surface roughness due to accelerated weathering. J Coat Technol Res. https://doi.org/10.1007/s11998-014-9634-3

13. Orellana JL, Wichhart D, Kitchens CL (2018) Mechanical and optical properties of polylactic acid films containing surfactant-modified cellulose nanocrystals. J Nanomat. https://doi.org/10.1155/2018/7124260

14. Zhu JY, Sabo R, Luo X (2011) Integrated production of nanofibrillated cellulose and cellulosic biofuel (ethanol) by enzymatic fractionation of wood fibers. Green Chem. https://doi.org/10.1039/C1GC15103G

15. Kong L, Xu D, He Z, Wang F, Gu S, Fan J, Pan X, Dai X, Dong X, Liu B, Li Y (2019) Nanocellulose-reinforced polyurethane for waterborne wood coating. Molecules. https://doi.org/10.3390/molecules24173151

16. Leenhouts F, Woud F (1978) Simple method of determining the birefringence of nematic liquid crystals. J Physique Let. https://doi.org/10.1051/jphyslet:019780039014024900

17. Jackson JD (1998) Classical electrodynamics. Willey, New York

18. Willard HH, Merritt LL, Dean JA, Settle FA (1981) Instrumental methods of analysis. Van Nostrand, New York

19. Niskanen I, Forsberg V, Zakrisson D, Reza S, Hummelgård M, Andres B, Fedorov I, Suopajärvi T, Liimatainen H, Thungström G (2019) Determination of nanoparticle size using Rayleigh approximation and Mie theory. Chem Eng Sci. https://doi.org/10.1016/j.ces.2019.02.020

20. Niskanen I, Räty J, Soetedjo H, Hibino K, Oohashi H, Heikkilä R, Matsuda K, Otani Y (2020) Measurement of the degree of polarisation of thermally modified Scots pine using a Stokes imaging polarimeter. Opt Rev. https://doi.org/10.1007/s10043-019-00572-w

21. Liimatainen H, Sirviö J, Haapala A, Hormi O, Niinimäki J (2011) Characterization of highly accessible cellulose microfibers generated by wet stirred media milling. Carbohyd Polym. https://doi.org/10.1016/j.carbpol.2010.11.007

22. Matsuo M, Umemura K, Kawai S (2012) Kinetic analysis of color changes in cellulose during heat treatment. J Wood Sci. https://doi.org/10.1007/s10086-011-1235-5

23. Macleod HA (2021) Thin-film optical filters. CRC Press, Boca Raton

24. Nilsson PO (1968) Determination of optical constants from intensity measurements at normal incidence. Appl Opt. https://doi.org/10.1364/AO.7.000435

25. Smith MH (2002) Optimization of a dual-rotating-retarder Mueller matrix polarimeter. Appl Opt. https://doi.org/10.1364/AO.41.002488

26. Sihtola H, Kyrklund B, Laamanen L, Palenius I (1963) Comparison and conversion of viscosity and DP values determined by different methods. Pap Puu 45:225–232

27. Ahn K, Zaccaron S, Zwirchmayr NS, Hettegger H, Hofinger A, Bacher M, Henniges U, Hosoya T, Potthast A, Rosenau T (2019) Yellowing and brightness reversion of celluloses: CO or COOH, who is the culprit? Cellulose. https://doi.org/10.1007/s10570-018-2200-x

28. Isogai A, Saito T, Fukuzumi H (2010) TEMPO-oxidized cellulose nanofibers. Nanoscale. https://doi.org/10.1039/C0NR00583E

29. Reid MS, Villalobos M, Cranston ED (2016) Cellulose nanocrystal interactions probed by thin film swelling to predict dispersibility. Nanoscale. https://doi.org/10.1039/C6NR01737A

30. Niskanen I, Heikkinen J, Mikkonen J, Harju A, Heräjärvi H, Venäläinen M, Peiponen KE (2012) Detection of the effective refractive index of thermally modified scots pine by immersion liquid method. J Wood Sci. https://doi.org/10.1007/s10086-011-1222-x

31. Uetani K, Koga H, Nogi M (2019) Estimation of the intrinsic birefringence of cellulose using bacterial cellulose nanofiber films. ACS Macro Lett. https://doi.org/10.1021/acsmacrolett.9b00024

32. Manaf MEA, Nitta KH, Yamgusci M (2016) Mechanical properties of plasticized cellulose ester films at room and high temperatures. ARPN J Eng Appl Sci 11(4):2354–2358

33. Degushi S, Tsujii K, Horikoshi K (2006) Cooking cellulose in hot and compressed water. Chem Commun. https://doi.org/10.1039/B605812D

34. Barbash VA, Yaschenko OV, Alushkin SV, Kondratyuk AS, Posudievsky OY, Koshechko VG (2016) The effect of mechanochemical treatment of the cellulose on characteristics of nanocellulose films. Nanoscale Res Lett. https://doi.org/10.1186/s11671-016-1632-1

35. Selkälä T, Sirviö JA, Lorite GS, Liimatainen H (2016) Anionically stabilized cellulose nanofibrils through succinylation pretreatment in urea–lithium chloride deep eutectic solvent. Chemsuschem. https://doi.org/10.1002/cssc.201600903

36. Abral H, Ariksa J, Mahardika M, Handayani D, Aminah I, Sandrawati N, Sugiarti E, Muslimin AN, Rosanti SD (2020) Effect of heat treatment on thermal resistance, transparency and antimicrobial activity of sonicated ginger cellulose film. Carbohyd Polym. https://doi.org/10.1016/j.carbpol.2020.116287

37. Zhao J, Zhang W, Zhang X, Zhang X, Lu C, Deng Y (2013) Extraction of cellulose nanofibrils from dry softwood pulp using high shear homogenization. Carbohyd Polym. https://doi.org/10.1016/j.carbpol.2013.05.050